

## **Dimensional Control of Sinter Hardened P/M Components**

by

François Chagnon  
Quebec Metal Powders Limited

and

Martin Gagné  
Rio Tinto Iron & Titanium Inc.-Technology

### **ABSTRACT**

Sinter hardened P/M parts exhibit high strength and apparent hardness after sintering without the need of subsequent quenching operation. Although sinter hardening eliminates the distortion often experienced during quenching, this technique requires a close dimensional control during sintering due to the difficulty of correcting the dimensions of hardened materials by post-sintering sizing or machining. Meeting dimensional tolerances can be achieved by either a close monitoring of the sintering parameters and/or the design of mix formulations (adjustment of the graphite and copper concentrations) that minimize size variations.

Many studies have been made to determine the mechanisms involved during sintering unalloyed powders with copper and graphite but there are only a few related to low alloy steel powders intended for sinter hardening where different phases (bainite, martensite and retained austenite) are produced on cooling. A dilatometry study was conducted to characterize the effects of admixed graphite and copper concentrations on the dimensional change of specimens made of sinter hardenable powders. Test specimens were pressed to  $6.9 \text{ g/cm}^3$  from mixes containing 0 to 2 % copper and the amount of graphite required to reach 0.35 to 0.95% combined carbon. Test pieces were sintered 25 minutes at  $1120^\circ\text{C}$  and cooled at a rate of  $0.1^\circ\text{C/s}$  in the temperature range of 650 to  $400^\circ\text{C}$ . Results were compared to values achieved with specimens pressed to the same density but sintered in mesh belt furnaces.

### **INTRODUCTION**

Sinter hardening is a process in which the martensitic transformation takes place when parts are cooled from the sintering temperature. Therefore, P/M parts achieve high hardness after sintering. The main benefits of sinter hardening are the elimination of secondary heat treatment operations, reduced distortion because of slower cooling rates than oil quenching and oil free parts. Base powders used for sinter hardening must however possess sufficient hardenability to prevent both pearlitic and bainitic transformations at the cooling rates (from 0.6 to  $1.5^\circ\text{C/s}$  in the temperature range of 600 to  $450^\circ\text{C}$ ) usually

observed with current sintering furnaces, depending on whether or not a fast cooling unit is used. Copper is also frequently admixed to further increase hardenability.

However, because of the high apparent hardness achieved after sintering, it is difficult to machine sinter hardened parts. Therefore, dimensional change becomes a key control variable to avoid parts rejection after sintering. It is well known that copper and graphite affect dimensional change of iron powders and many studies have been made to characterize the diffusion mechanisms involved during sintering [1, 2, 3]. However, only a few investigations have been carried out specifically addressing low alloy steel powders [4, 5] where bainite and martensite are produced during cooling along with retained austenite [6, 7, 8]. In a previous study [7], it has been found that dimensional change of sinter hardening powders can be very sensitive to variations in carbon content, particularly with 2% admixed copper. As illustrated in Figure 1, the range of dimensional change as a function of carbon content is larger with sinter hardenable low alloy steel powder, ATOMET 4701, than with unalloyed powder (ATOMET 1001), indicating that the material formulation is key in achieving the required dimensional tolerances with hardened parts.

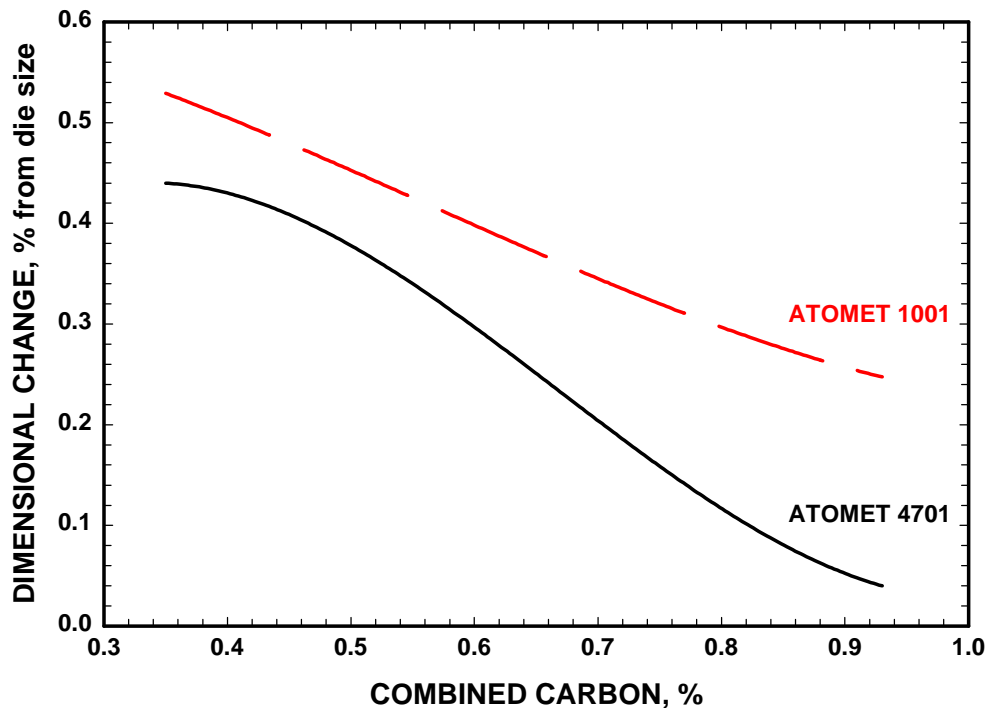


Figure 1. Effect of carbon content on dimensional change from die size of specimens pressed from mixes based on ATOMET 4701 and ATOMET 1001 and containing 2% Cu, sintered 25 minutes at 1120°C (sintered density: 6.8 g/cm<sup>3</sup>) [7, 9].

Therefore, the objective of this study is to determine the effect of admixed graphite and copper on the sintering mechanisms of low alloy steel powders designed for sinter hardening applications and to relate them to the results observed in production sintering furnaces.

### **EXPERIMENTAL PROCEDURE**

ATOMET 4701, a Fe-0.45Mn-0.45Cr-1.0Mo-0.9Ni low alloy steel powder, was used as base material for this study. Mixes containing 0.75% zinc stearate were prepared with various additions of graphite and copper as reported in Table 1.

One inch long by 0.25 inch wide and 0.2 inch thick specimens were pressed to 6.9 g/cm<sup>3</sup> and heat treated at 600°C to burn off the lubricant. Dilatometric measurements were carried out with a Theta Dilatronic dual push rod dilatometer in an inert atmosphere. The sintering temperature was 1120°C with a holding time at temperature of 25 minutes. Figure 2 illustrates the temperature profile used in this work. The heating rate to the sintering temperature was 9°C/min. while the cooling rate was 6°C/min. (0.1°C/s) in the range of 650 to 400°C. This cooling rate is significantly lower than that usually observed in industrial furnaces but was required to prevent failure of the ceramic parts of the dilatometer.

Table 1  
Mix compositions used in this study.

| Mix number | Graphite, % | Copper, % |
|------------|-------------|-----------|
| 1          | 0.50        | 0         |
| 2          | 0.90        | 2         |
| 3          | 1.10        | 0         |
| 4          | 0.50        | 1         |
| 5          | 0.90        | 0         |
| 6          | 1.10        | 1         |
| 7          | 0.50        | 2         |
| 8          | 0.90        | 1         |
| 9          | 1.10        | 2         |

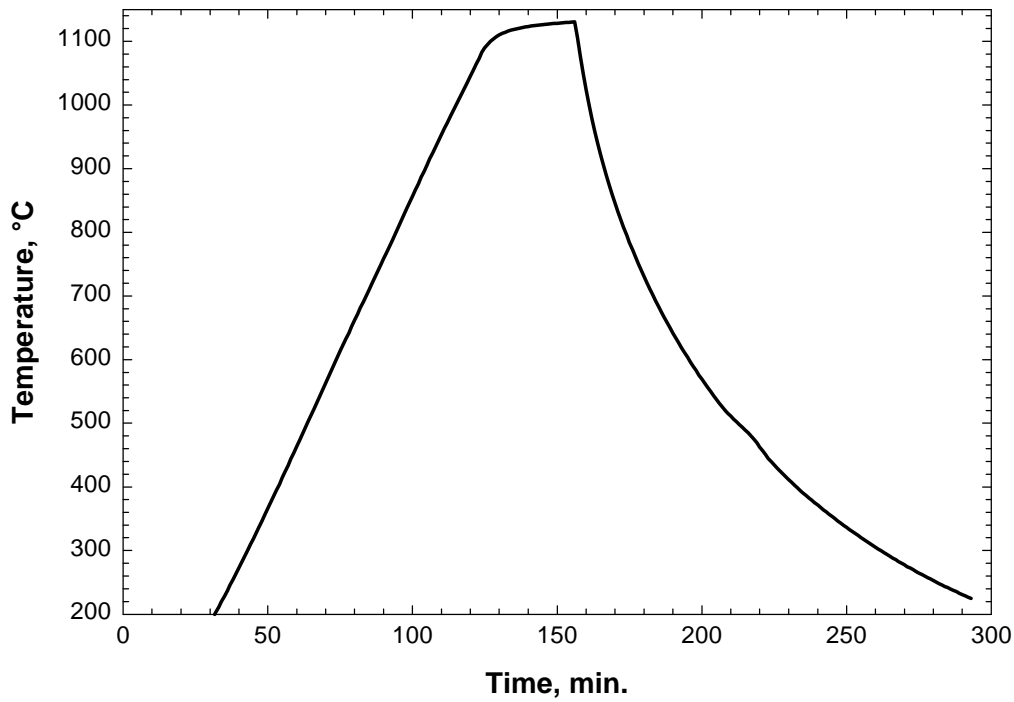


Figure 2. Temperature profile used for the dilatometric studies.

## RESULTS AND DISCUSSION

### Dilatometry characterization

Figures 3, 4 and 5 illustrate the dilatometry profiles of specimens pressed to  $6.9 \text{ g/cm}^3$  and containing 0.35, 0.70 and 0.95% C and 0, 1 and 2% copper, respectively. Up to about  $650^\circ\text{C}$ , specimens expand similarly as the temperature increases. The expansion rate,  $0.00148 \text{ \%/}^\circ\text{C}$ , corresponds to the thermal expansion coefficient of ferrite. At about  $750^\circ\text{C}$ , the expansion rate decreases and the specimens shrink in the temperature range of 800 to  $950^\circ\text{C}$ . This is the temperature range of the  $\alpha$  to  $\gamma$  transformation. This phase transformation takes place over a wide range of temperatures because a small quantity of carbon diffuses in the iron lattice [10]. At  $950^\circ\text{C}$  and above, the diffusion of carbon is accelerated. It is worth noting that, as shown by the increasing slope of the dilatometric curves in the  $950\text{-}1050^\circ\text{C}$  temperature range, and as summarized in Figure 6, the specimen expansion increases with the concentrations of carbon and copper.

It is also observed that the expansion related to copper melting at about  $1080^\circ\text{C}$ , the melting point of copper, is detected only at the lowest carbon concentration, 0.35%, and increases from about 0.06 to 0.25% as the copper content is raised from 1 to 2%. This indicates that copper in specimens containing 0.70% C or more does not penetrate the steel grain boundaries. This result is in accordance with previous studies carried out with iron powders [1], which show that carbon increases the dihedral angle of liquid copper and inhibits its penetration in the iron skeleton.

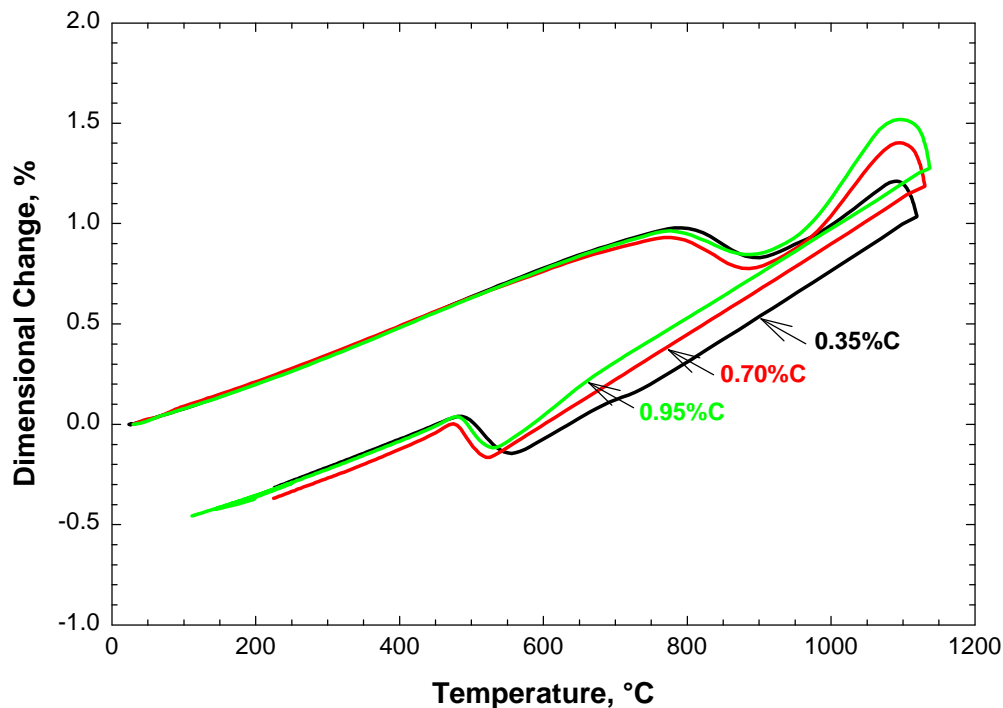


Figure 3. Dilatometry profiles of copper free specimens containing respectively 0.35, 0.7 and 0.9% combined carbon (green density:  $6.9 \text{ g/cm}^3$ ).

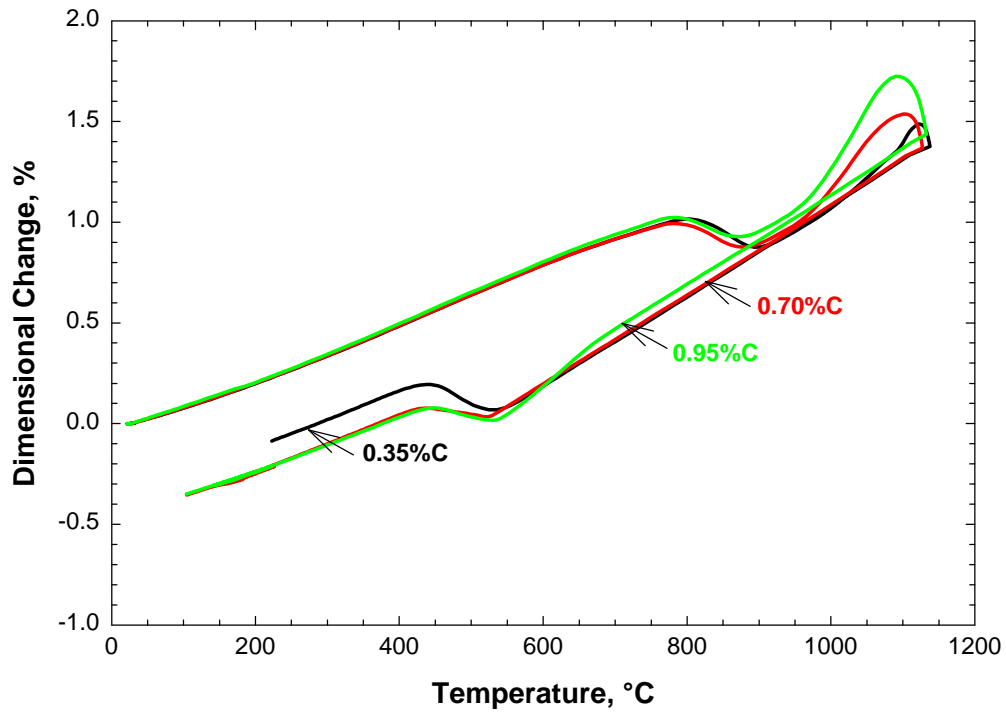


Figure 4. Dilatometry profiles of specimens containing 1% Cu and, respectively, 0.35, 0.7 and 0.9% combined carbon (green density: 6.9 g/cm<sup>3</sup>).

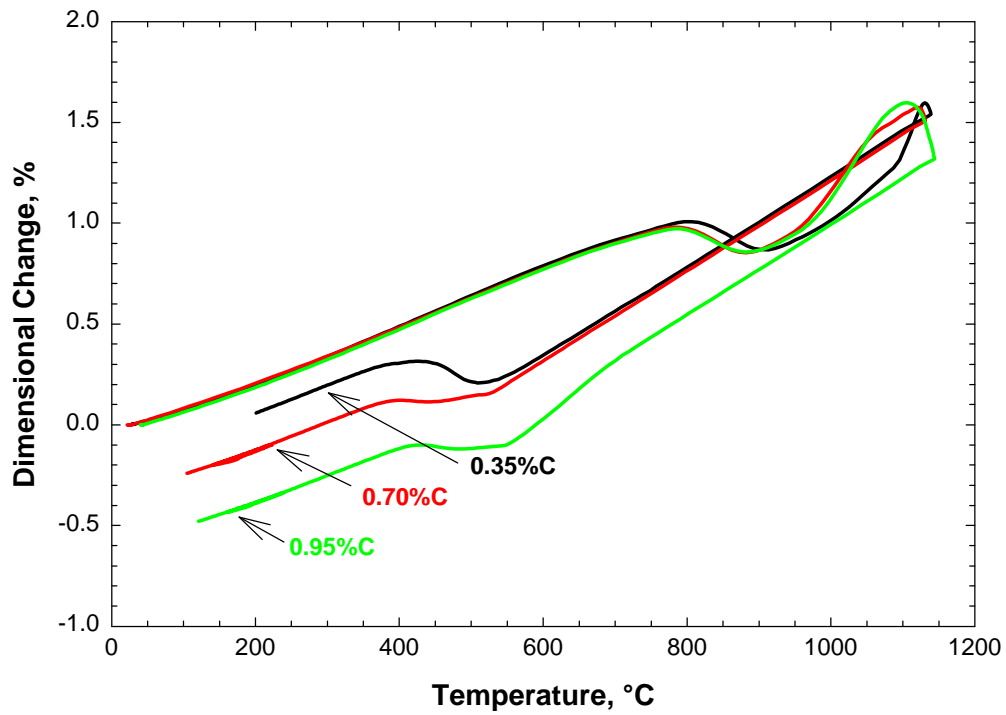


Figure 5. Dilatometry profiles of specimens containing 2% Cu and, respectively, 0.35, 0.7 and 0.9% combined carbon (green density: 6.9 g/cm<sup>3</sup>).

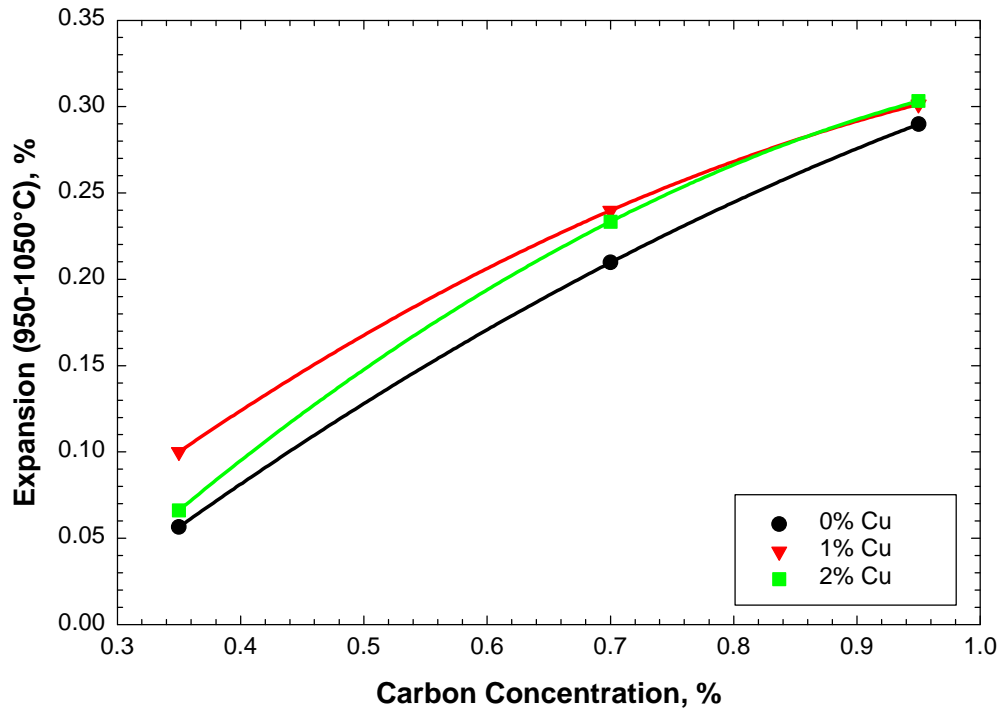


Figure 6. Specimen expansion due to carbon diffusion in the temperature range of 950 to 1050°C.

Shrinkage occurs during isothermal sintering at 1120°C, the amplitude of the shrinkage varies with the carbon and copper contents as shown in Figure 7. In copper free materials, shrinkage slightly increases with the carbon concentration and the rate of contraction is larger at high carbon content indicating that carbon favors densification. Below 0.70% C, shrinkage decreases with the addition of copper, because copper diffuses in iron and reduces the isothermal shrinkage [3]. At 0.95% C, the isothermal shrinkage is comparable for materials containing 1 and 2% Cu and is similar to that of copper free alloy, meaning that activated sintering due to carbon counteracts the volume expansion due to the diffusion of copper.

When cooling from 1120 to 750°C, the contraction rate is similar for the various alloys i.e. 0.0025%/°C, and corresponds to that of the thermal expansion coefficient of austenite. However, the specimen containing 0.35% C without copper, Figure 2, shows a slight expansion at about 730°C. This expansion can be related to the initiation of the  $\gamma$ - $\alpha$  transformation. The end of transformation takes place at about 480°C. It is also worth noting a contraction of the specimen containing 0.95% C from 650 to 550°C. The same behavior is observed for the specimens containing 0.95% C and 1% Cu and 2% Cu with carbon contents of 0.7 and 0.95%. This contraction could be the result of carbide precipitation because of the very slow cooling rate combined with the hypereutectoid composition of these alloys. As seen in Figure 8, the presence of cementite particles validates this assumption.

For the other alloys, the  $\gamma$ - $\alpha$  transformation which causes the specimens to expand, takes place in the range of 540 to 480°C. Figure 9 illustrates the effect of carbon and copper contents on the expansion during this phase transformation. The expansion of the specimens decreases with raising carbon content for the various copper concentrations but the expansion rate is lower in the copper free materials. This reduction of specimen expansion during the  $\gamma$ - $\alpha$  transformation with increasing carbon content is probably the result of a decrease in the amount of pearlite produced to the benefit of bainite. This is also confirmed by the microstructures shown in Figure 10, where the amount of bainite increases with the carbon and copper concentrations.

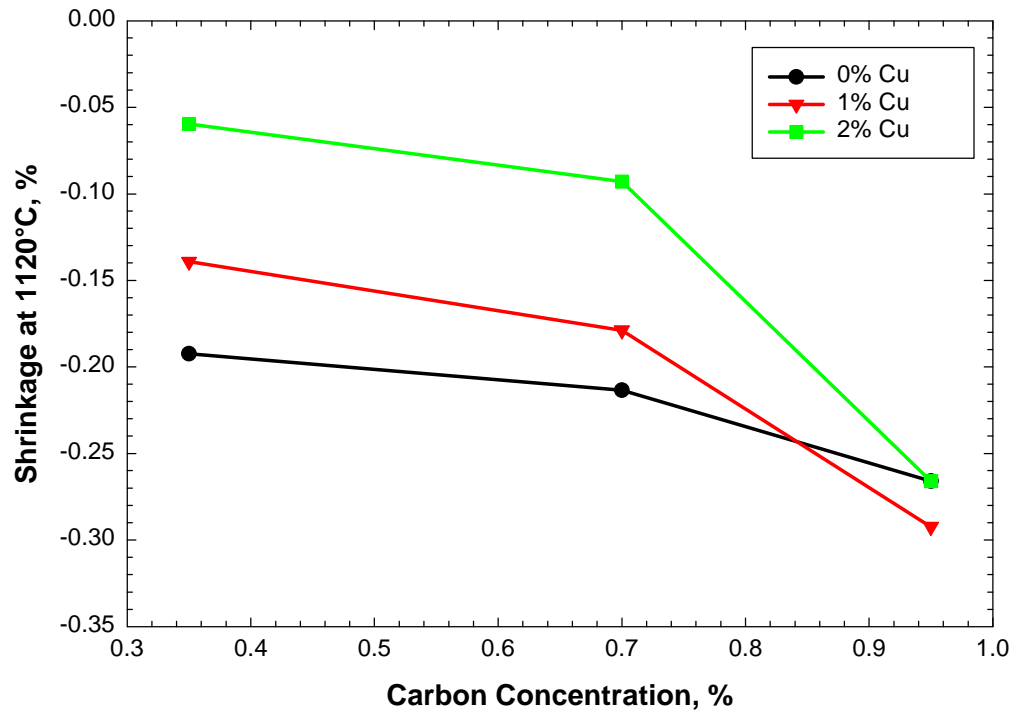


Figure 7. Effect of carbon and copper on dimensional change during the isothermal sintering of 25 minutes at 1120°C.

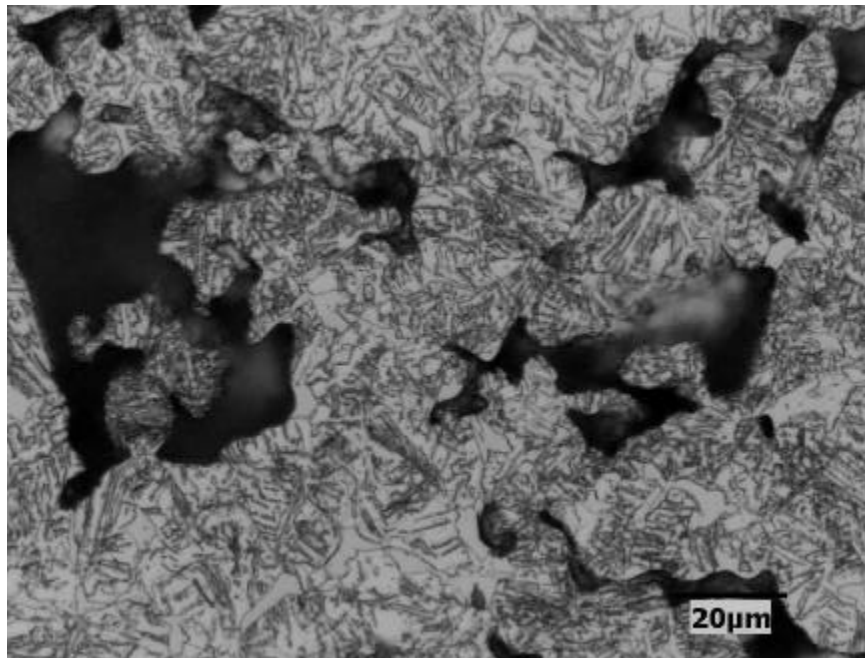


Figure 8. Microstructure of a specimen containing 0.95% C and 1% Cu cooled at 0.1°C/s.

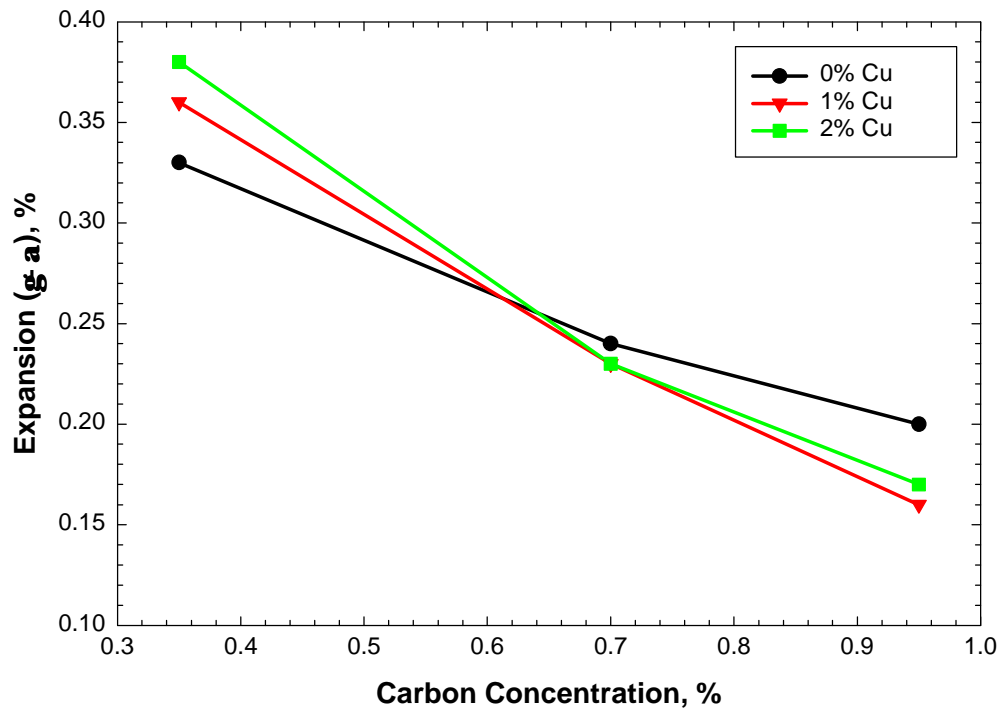


Figure 9. Specimen expansion measured during the phase transformation  $\gamma$ - $\alpha$  for the various levels of carbon and copper.

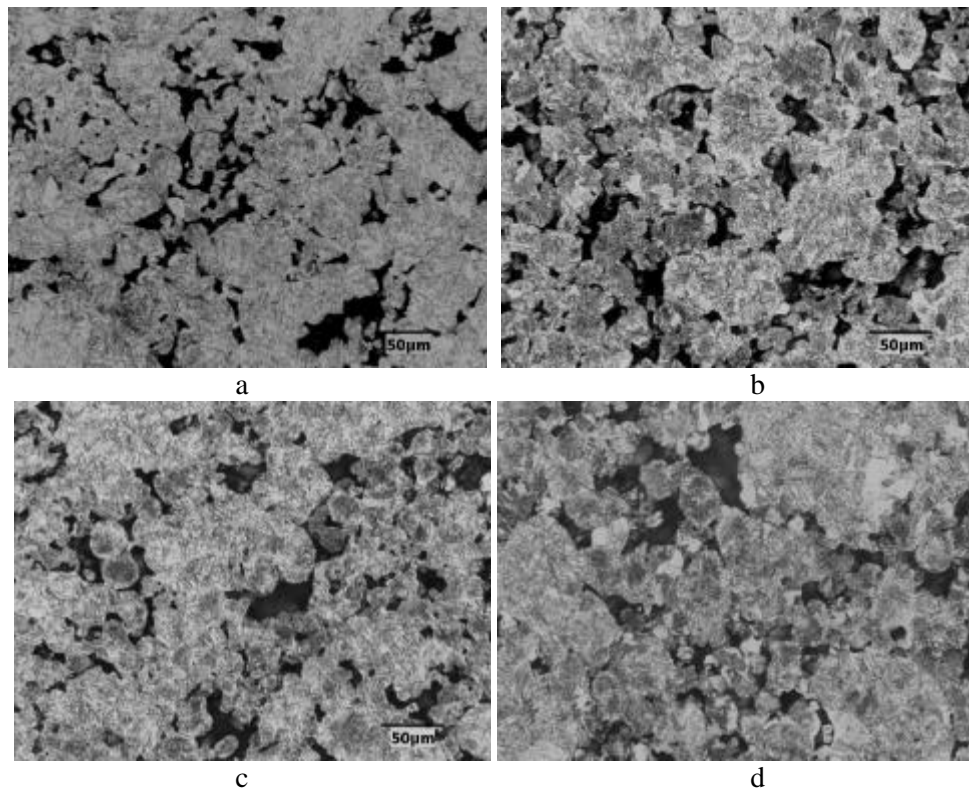


Figure 10. Microstructure of specimens with 0.95% C (a), 0.70% C+1% Cu (b), 0.95% C+1% Cu (c) and 0.70% C+2% Cu (d), cooled at 0.1°C/s.

### Comparison with unalloy steel powders

Figure 11 shows the dilatometry profiles of a FC-0205 (0.65% C) material and that of sinter hardening low alloy steel with 2% Cu and 0.70% C. The main differences can be summarized as follows:

- Carbon diffuses at lower temperature in the unalloyed powder.
- There is a larger expansion due to the melting of copper at about 1080°C with the unalloyed powder. There is no evidence of copper penetration at the grain boundaries with the low alloy powder.
- Slight larger shrinkage is observed during the isothermal sintering with unalloyed powders.
- The  $\gamma$ - $\alpha$  transformation occurs at higher temperature with the unalloyed powder, 700-650°C versus 550-480°C for the low alloy powder.
- The  $\gamma$ - $\alpha$  transformation of the unalloyed steel powder results in a larger expansion than that of the low alloy steel powder.

When cooling begins, both materials show similar dimensional changes. However, due to a larger expansion during the  $\gamma$ - $\alpha$  transformation, the specimen pressed from unalloyed powder ends with a dimension about 0.15% larger than that of the one prepared from low alloy steel powder. This difference is similar to that observed in Figure 1 for a specimen containing 0.7% C.

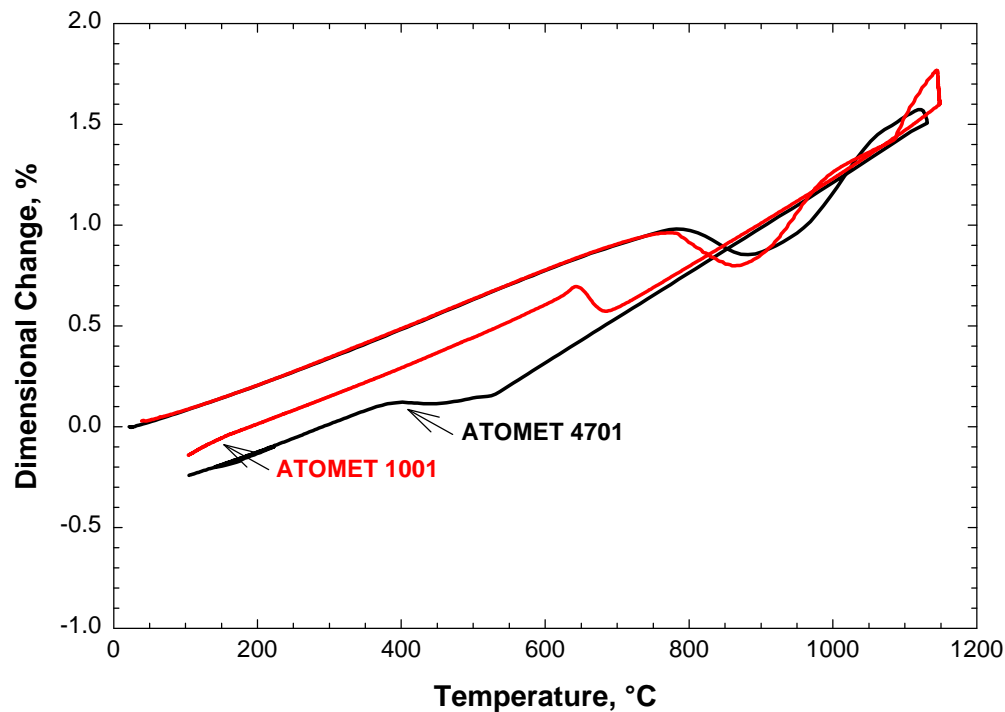


Figure 11. Dilatometry profiles of specimens containing 0.65-0.70% C and 2% Cu made from unalloyed (ATOMET 1001) and low alloy steel (ATOMET 4701) powders.

## Dimensional and hardness control versus carbon and copper contents

In a previous study [7], the effect of carbon and copper on dimensional change was evaluated for cooling rates of 0.4 and 1.5°C/s in the temperature range of 650 to 400°C. As shown in Figure 12, for both cooling rates and a 2% Cu addition, the dimensional change is very sensitive to a variation of combined carbon, particularly in the range of 0.4 to 0.95%. However, at 1% Cu, the dimensional change of specimens is significantly less variable with a change of the carbon content. As shown in Figure 4, at 1% Cu, the specimens expansion due to carbon and copper diffusion is compensated by a larger shrinkage during isothermal sintering at 1120°C, resulting in almost similar dimensions after sintering. The difference in dimensions at room temperature is then only controlled by the phase transformations during cooling. At 2% Cu, Figure 5, the 0.95% C specimen shrinks significantly more than the others and this difference is greater when the phase transformations occur cooling. It is worth noting that these results were obtained with a slow cooling rate of 0.1°C/s, forming pearlite and bainite. For accelerated cooling, up to 90% martensite can be achieved, depending on the carbon and copper concentrations [7]. However, at high carbon contents, the amount of retained austenite can increase up 30% to the detriment of martensite [7]. Therefore, the specimens expand as the amount of martensite increases but this growth can be offset if a large quantity of retained austenite is present.

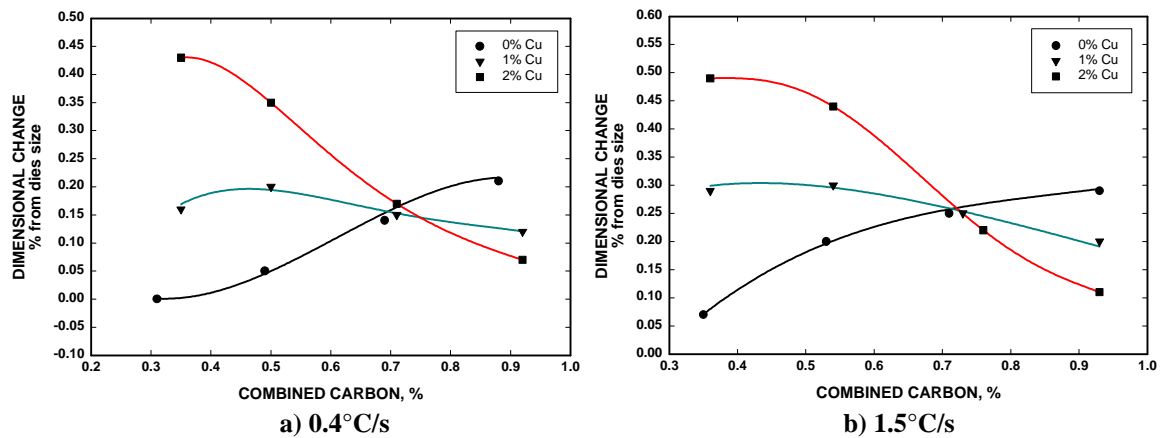


Figure 12. Evolution of dimensional change from die size as a function of combined carbon and copper concentrations for cooling rates of a) 0.4°C/s and b) 1.5°C/s in the temperature range of 650 to 400°C (green density: 6.9 g/cm<sup>3</sup>) [7].

In addition to dimensional control, a key parameter of sinter hardenable materials is to reach high apparent hardness in the as-sintered condition. Figure 13 illustrates the effect of material composition and post-sintering cooling rate on apparent hardness of specimens prepared from ATOMET 4701. With an addition of 1% admixed copper and a cooling rate of 0.4°C/s in the range of 605 to 450°C, a combined carbon larger than about 0.60% is required to achieve apparent hardness values superior to 30 HRC. Slightly higher values can be achieved with a 2% copper addition but this will be obtained at the detriment of the dimensional control. Increasing the cooling rate to 1.5°C/s raises the apparent hardness values by about 10 HRC (vis-à-vis specimens cooled at 0.4°C/s) and also widens the carbon range where stable hardness values can be maintained.

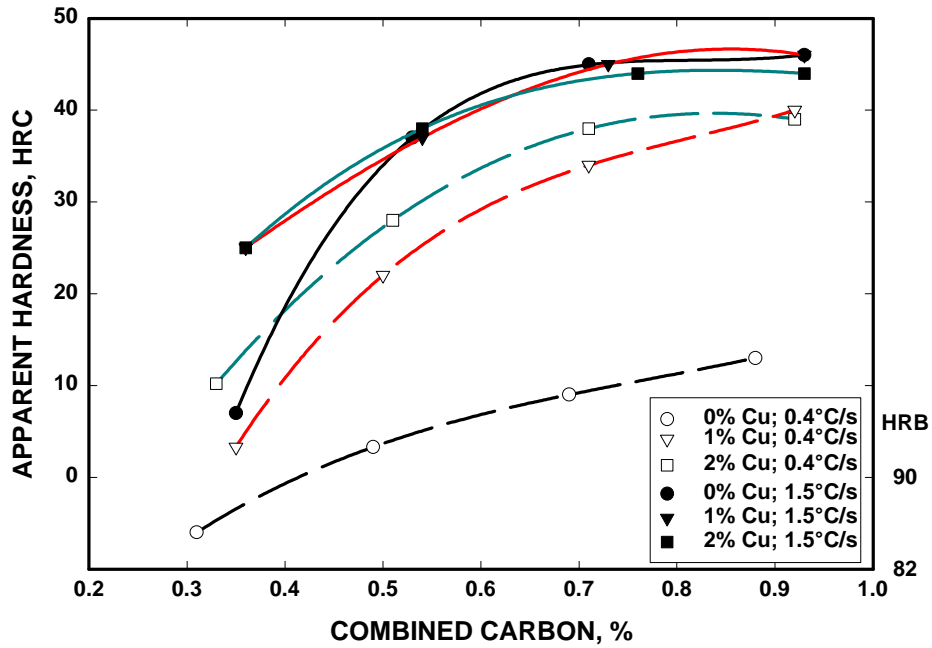


Figure 13. Evolution of apparent hardness as a function of combined carbon and copper concentration for cooling rates of a) 0.4°C/s and b) 1.5°C/s in the temperature range of 650 to 400°C (green density: 6.9 g/cm<sup>3</sup>) [7].

## CONCLUSIONS

Tests were carried out with a dilatometer to study the sintering mechanisms affecting the dimensional change that takes place during sintering and cooling specimens pressed from sinter hardenable powders (ATOMET 4701). The main conclusions that can be drawn from this study are:

1. An expansion of the specimens due to the diffusion of carbon is observed in the temperature range of 950 to 1050°C. This expansion increases with the carbon content and occurs over a wider range of temperatures compared to unalloyed steel powder.
2. Growth due to the melting of copper at about 1080°C is evident only at low carbon content i.e 0.35%, for specimens made from ATOMET 4701, while it is also observed at 0.7% C for specimens pressed from unalloyed steel powder.
3. Shrinkage during isothermal sintering at 1120°C increases with carbon content for copper concentrations in the range of 0 to 2%. Below 0.9% C, a larger shrinkage is observed as the copper content decreases while at 0.95%, the shrinkage is similar regardless of the copper concentration.
4. At a cooling rate of 0.1°C/s, precipitation of carbides is observed at 0.95% C whatever the copper concentration and in the material containing 0.7% C and 2% Cu. This is related to the hypereutectoid composition of these alloys and the slow cooling rate after sintering.
5. The  $\gamma$ - $\alpha$  transformation in specimens made of ATOMET 4701 takes place at lower temperature than in specimens made of unalloyed steel powder. Also, the expansion is reduced as the amount of pearlite decreases while that of bainite increases.

6. Dimensional change of specimens pressed from ATOMET 4701 is less sensitive to carbon variation at 1% copper since the expansion due to the diffusion of carbon and copper is offset by the larger shrinkage at the sintering temperature.

## **REFERENCES**

1. Y. Trudel and R. Angers, Comparative Study of Fe-Cu-C Alloys Made from Mixed and Prealloyed Powders, Modern Development in Powder Metallurgy, Metal Powder Industries Federation, Princeton, 1973, pp. 305-322.
2. N. Dautzenberg and H.J. Dorweiler, Dimensional Behaviour of Copper-Carbon Sintered Steels, Powder Metallurgy International, Vol. 17, no. 6, 1995 pp.279-282.
3. A. Griffo, J. Ko and R.M. German, Critical Assessment of Variables Affecting the Dimensional Behavior in Sintered Iron-Copper-Carbon Alloys, Advances in Powder Metallurgy & Particulate Materials, Metal Powder Industries Federation, Princeton, 1994, vol. 3, pp. 221-233.
4. P. François and E. Gautier, Sintering Behaviour of 4401 Based Alloy, Advances in Powder Metallurgy & Particulate Materials, Metal Powder Industries Federation, Princeton, 1996, vol. 3, pp. 11-329 to 11-341.
5. R.W. Kiefer, Jr.L. Ceci and Y. Chen, A Study of Dimensional Change in a Sinter Hardening Alloy Steel, Advances in Powder Metallurgy & Particulate Materials, Metal Powder Industries Federation, Princeton, 1993, vol. 2, pp. 133-151.
6. F. Chagnon and G. Olschewski, Low Alloy Steel Powders for Sinter Hardening Applications, Proceeding of 2000 Powder Metallurgy World Congress, The Japan Society of Powder and Powder Metallurgy, Kyoto, 2000, part 2, p. 927-930.
7. F. Chagnon and M. Gagné, Effect of Graphite and Copper Concentrations and Post Sintering Cooling Rate on Properties of Sinter Hardened Materials, Advances in Powder Metallurgy & Particulate Materials, Metal Powder Industries Federation, Princeton, 2000, part 13, pp. 13-37 to 13-47.
8. G. L'Espérance, S. Martel, A. de Rege, B. Kiefer and Y.T. Chen, Evaluation of the Effect of Tempering on Microstructure and Properties of Three Widely Used Sinter Hardening Alloys, Advances in Powder Metallurgy & Particulate Materials, Metal Powder Industries Federation, Princeton, 1995, vol. 2, pp. 8-39 to 8-54.
9. QMP data sheet, ATOMET 1001.
10. F. Chagnon and M. Gagné, Machining Sinter Hardenable P/M Materials, Proceeding of 1998 Powder Metallurgy World Congress, EPMA, Granada, 1998, pp. 384-389.